

#### ASME Journal of Offshore Mechanics and Arctic Engineering Online journal at:

https://asmedigitalcollection.asme.org/offshoremechanics



# Taiyu Zhang

Institute for Ocean Engineering, Tsinghua University, Shenzhen 518055, China e-mail: taiyu.zhang@outlook.com

#### Can Ma

Institute for Ocean Engineering, Tsinghua University, Shenzhen 518055, China e-mail: c-ma21@mails.tsinghua.edu.cn

# Shangyuan Chen

Naval Research Institute, Beijing 100071, China e-mail: ahsscsy@126.com

# Zhengru Ren<sup>1</sup>

Assistant Professor Institute for Ocean Engineering, Tsinghua University, Shenzhen 518055, China e-mail: zhengru.ren@sz.tsinghua.edu.cn

# Enhanced Wave Buoy Analogy Through Heading Adjustment Strategy Based on Restricted Isometry Property

The safety and efficiency of marine operations are significantly influenced by external environmental conditions, with waves being the most critical factor affecting floating structures. These waves are described by the directional wave spectrum, which includes both spatial and frequency power distributions. However, real-time in situ wave spectrum measurements are often insufficient due to limitations in traditional methods. To address this issue, the wave buoy analogy (WBA) has emerged as a cost-effective and viable method for estimating sea states using ship motion responses. Despite its potential, the performance of WBA can vary due to a ship's inherent hydrodynamic properties, specifically response amplitude operators (RAOs). This variability can lead to inaccurate sea state estimations, posing potential risks. In this study, an adaptive ship heading adjustment strategy was proposed to enhance the accuracy of WBA by identifying optimal heading angles, thereby mitigating inaccuracies in specific sea states. The WBA performance can be preliminarily evaluated from the perspective of restricted isometry property (RIP) using RAOs as input. The received assessment criterion helps determine the direction in which the ship can provide a more accurate estimate. The implementation of the heading adjustment strategy significantly improves the accuracy and robustness of sea state estimations. Numerical simulations validate the effectiveness of the proposed algorithm. [DOI: 10.1115/1.4068177]

Keywords: sea state estimation, wave buoy analogy, restricted isometry property, ship heading adjustment

#### 1 Introduction

External environmental information is of paramount importance in supporting various offshore operations [1–4]. Among the external loads, waves exert the most pronounced influence on marine structures. Consequently, accurately estimating the on-site sea state becomes imperative for facilitating real-time decision-making, thereby ensuring operational efficiency and reliability [5]. Given the limitations inherent in conventional estimation approaches, including meteorological satellite systems, wave rider buoys, and shipborne wave radar, wave buoy analogy (WBA) has emerged as a cost-effective solution. Utilizing the WBA, oscillating ships can be regarded as large wave buoys, providing nearly real-time wave information [6].

Categorically, the WBA can be divided into model-based approaches and data-driven approaches, contingent on the necessity of the transfer functions, i.e., response amplitude operators (RAOs). Within the model-based WBA, it is assumed that the RAOs are perfectly known and can precisely represent the linear relationship between ship responses and waves in the frequency domain [7].

The optimal wave spectra or environmental parameters are then calculated by solving the inverse problem. Bayesian modeling is employed for sea state estimation, involving iterative updates of prior information and posterior inference [8–10]. Adaptive Kalman filter is introduced to provide a recursive solution for real-time sea states [11–13]. Sparse regression is a prevalent method for addressing such inverse problems to handle cross-response spectra with disturbance, offering a nonparametric solution [14,15]. However, in the model-based WBA, the accuracy of a transfer function is crucial. Satellite altimeter observations are utilized to calibrate the RAO and minimize errors, thereby improving the accuracy and robustness of the WBA [16,17].

Conversely, the data-driven WBA endeavors to estimate wave information through the utilization of either online or offline training models, aiming to reduce the reliance on the RAOs. Data-driven methods are employed for sea state classification and estimation based on ship responses [18,19]. State-of-the-art artificial intelligence frameworks are also introduced to provide enhanced estimates, free from the hydrodynamic model [20–22]. Nevertheless, the constraints posed by the scarcity of training data and the high computational costs must be considered.

The unevenly distributed RAOs make it challenging for the estimates from WBA to remain consistently accurate due to the inherent geometry of vessels. The inaccuracy can be theoretically attributed to two main aspects: erroneous measurement of response cross-spectra and numerical instability encountered in solving

<sup>&</sup>lt;sup>1</sup>Corresponding author.

Contributed by the Ocean, Offshore, and Arctic Engineering Division of ASME for publication in the Journal of Offshore Mechanics and Arctic Engineering. Manuscript received June 18, 2024; final manuscript received March 5, 2025; published online April 3, 2025. Assoc. Editor: Bing Ren.

inverse problems. In our early work, the restricted isometry property (RIP) has proven effective in elucidating performance variations in WBA, offering a preliminary evaluation based solely on the ship's RAOs [23]. In this study, we propose an adaptive strategy to adjust the ship heading based on the identification of the main characteristics of incoming waves and the RIP criteria. This adjustment of the ship's heading aids in avoiding inaccurate measurements of response spectra. Furthermore, the introduction of RIP is employed to pinpoint the optimal angle of adjustment, thereby enhancing the accuracy of sea state estimation.

The main contributions of this paper are as follows:

- The RIP is introduced into the WBA to a provide preevaluation of the performance based on RAOs.
- (2) The heading adjustment strategy is proposed to avoid the erroneous measurement of response spectra and performance deterioration of WBA.

This study is organized as follows. Section 2 outlines the formulation of the WBA problem and the associated challenges. In Sec. 3, the heading adjustment strategy is introduced. Simulation results are illustrated in Sec. 4. Finally, Sec. 5 concludes the paper.

#### 2 Problem Formulation

**2.1 Wave Buoy Analogy.** In the present study, a stationkeeping scenario is considered, where a dynamic positioning (DP) vessel maintains its position and heading while oscillating in sea waves. Assumptions include the perfect knowledge of RAOs, and a stable sea state is maintained throughout the sampling period. Heave, roll, and pitch motions are taken into account because the influence of the DP system can be neglected, indexed by the set  $\mathbb{I} = \{3, 4, 5\}$ . The directional wave spectrum to be estimated is discretized into a network with the size of  $N_{\omega} \times N_{\beta}$ . The ship heading  $\psi$  represents the angle of the longitude ship axis relative to the North. The wave heading direction  $\beta$  describes the wave direction with respect to the ship heading. The definition of the established coordinate system and the wave characteristics from different incoming angles are presented in Fig. 1.

In the WBA, the ship is considered a linear time-invariant system, featuring a linear correlation between the cross-spectra of ship

motions and the real-time wave spectrum. The RAOs are complex transfer functions of this system. The mathematical expression for the response cross-spectra at frequency  $\omega_m$  involves an integral over the entire range of wave headings and yields

$$S_{ij}(\omega_m) = \int_{-\pi}^{\pi} \Phi_i(\omega_m, \beta) \overline{\Phi_j(\omega_m, \beta)} E(\omega_m, \beta) \, \mathrm{d}\beta$$

$$\approx \Delta \beta \sum_{n=1}^{N_\beta} \Phi_i(\omega_m, \beta_n) \overline{\Phi_j(\omega_m, \beta_n)} E(\omega_m, \beta_n) \tag{1}$$

where S,  $\Phi$ , and E represent the response cross-spectra, transfer functions, and wave spectrum, respectively, with subscripts  $i, j \in \mathbb{I}$  denoting the indices of degrees-of-freedom (DOFs), and  $\Delta \beta$  is the interval between discrete directions. Equation (1) can be decomposed into three components with different permutations of DOFs. By combining equations across all frequencies, the mathematical expression for the WBA system can be reformulated in a matrix form, given by

$$b = Af \tag{2}$$

where b and f denote response spectra and directional wave spectrum in a vector form, and A is the transfer matrix containing RAO information. Hereafter, the estimation of real-time sea state transforms into solving an ill-posed problem, entailing numerical challenges such as the lack of a unique solution and susceptibility to perturbations.

**2.2 Nonparametric Estimation Through Convex Optimization.** To address the problem, convex optimization is employed in this study and directly provides a nonparametric estimation of the wave spectrum. The sparsity and smoothness inherent in the physical characteristics of the wave spectrum are incorporated into the regression model, resulting in the cost function expressed as

$$\begin{split} \hat{f} &= \arg & \min_{f} & \|Af - b\|_{2}^{2} + \gamma_{1} \|f\|_{2}^{2} + \gamma_{2} \|Df\|_{1} \\ \text{s.t.} & f \geq 0 \\ f_{1} &= 0 \\ f_{N_{\omega}} &= 0 \end{split} \tag{3}$$

where  $\hat{f}$  denotes the optimum estimate that minimizes the cost function, D is the differential matrices capable of providing the

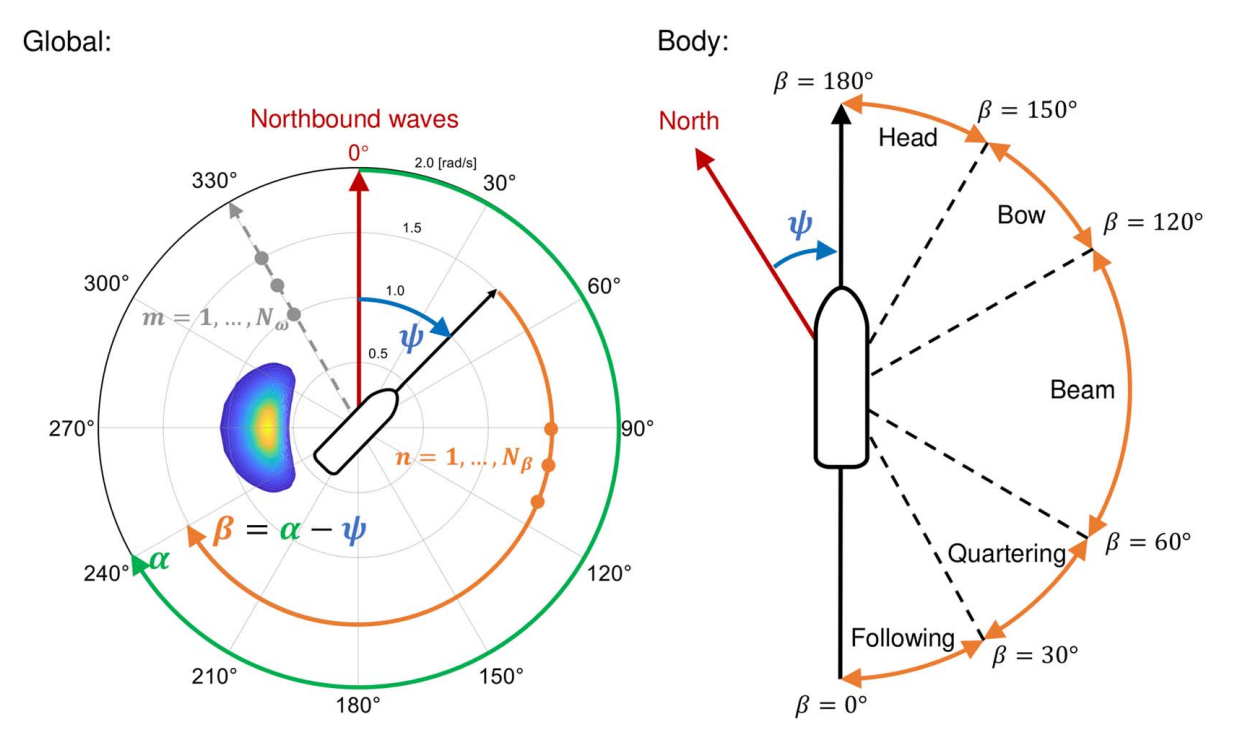


Fig. 1 Definition of the coordinate system and the encountered wave characteristic

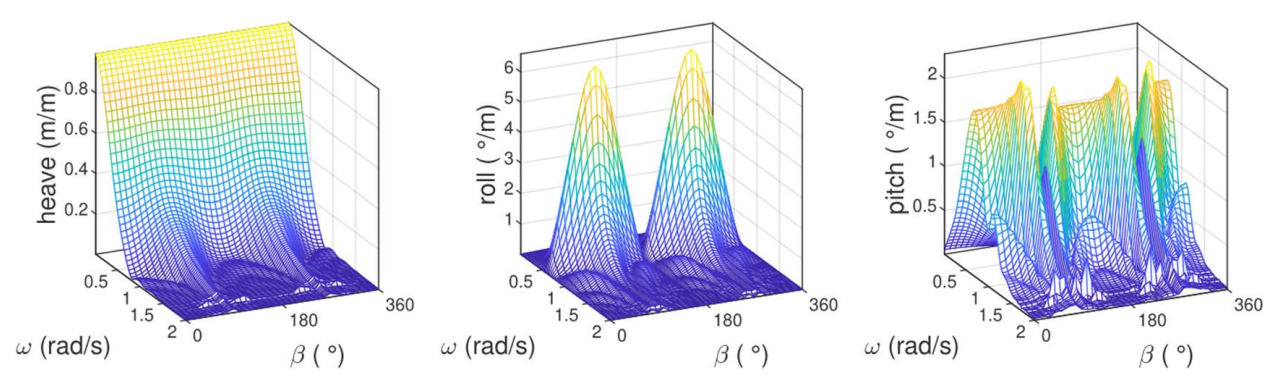


Fig. 2 RAOs of a cargo ship

second-order differences of f which are used to tune the smoothing terms, and  $\gamma_1$  and  $\gamma_2$  are penalty parameters ensuring a trade-off among residual, sparsity, and smoothness. Solutions that lack smoothness and sparsity are less likely to be accepted in the regression process. Consequently, the optimization results demonstrate sparsity and smoothness, achieved by selecting appropriate tuning parameters. Additional nonnegative constrains are taken into account due to the fact of a power spectrum. The estimated directional wave spectrum, denoted as  $\hat{E}$ , can be derived by reshaping the vector form  $\hat{f}$  into matrix form.

**2.3** Power Leakage of the Cross-Response Spectra. WBA relies significantly on the transformation of motion signals to the

frequency domain. The Welch procedure is utilized in this study to assess the cross-response spectra. By selecting a 60-s window with a 3/4 overlapping length, accurate response spectra can be obtained in most cases. When ships are on special courses, however, power leakage can occur because of inadequate response excitation within a limited sampling period. As the RAOs of a cargo ship are illustrated in Fig. 2, roll motion has nearly no response in heading seas and following seas and pitch motion exhibits low response in beam seas.

The ideal cross-spectra, obtained from Eq. (2) through the multiplication of the transfer matrix A and the predefined wave spectrum f, are compared with the measured cross-spectra (refer to Fig. 3). Notably, in the following seas (first row), the power of roll motion is significantly low, while heave and pitch motions

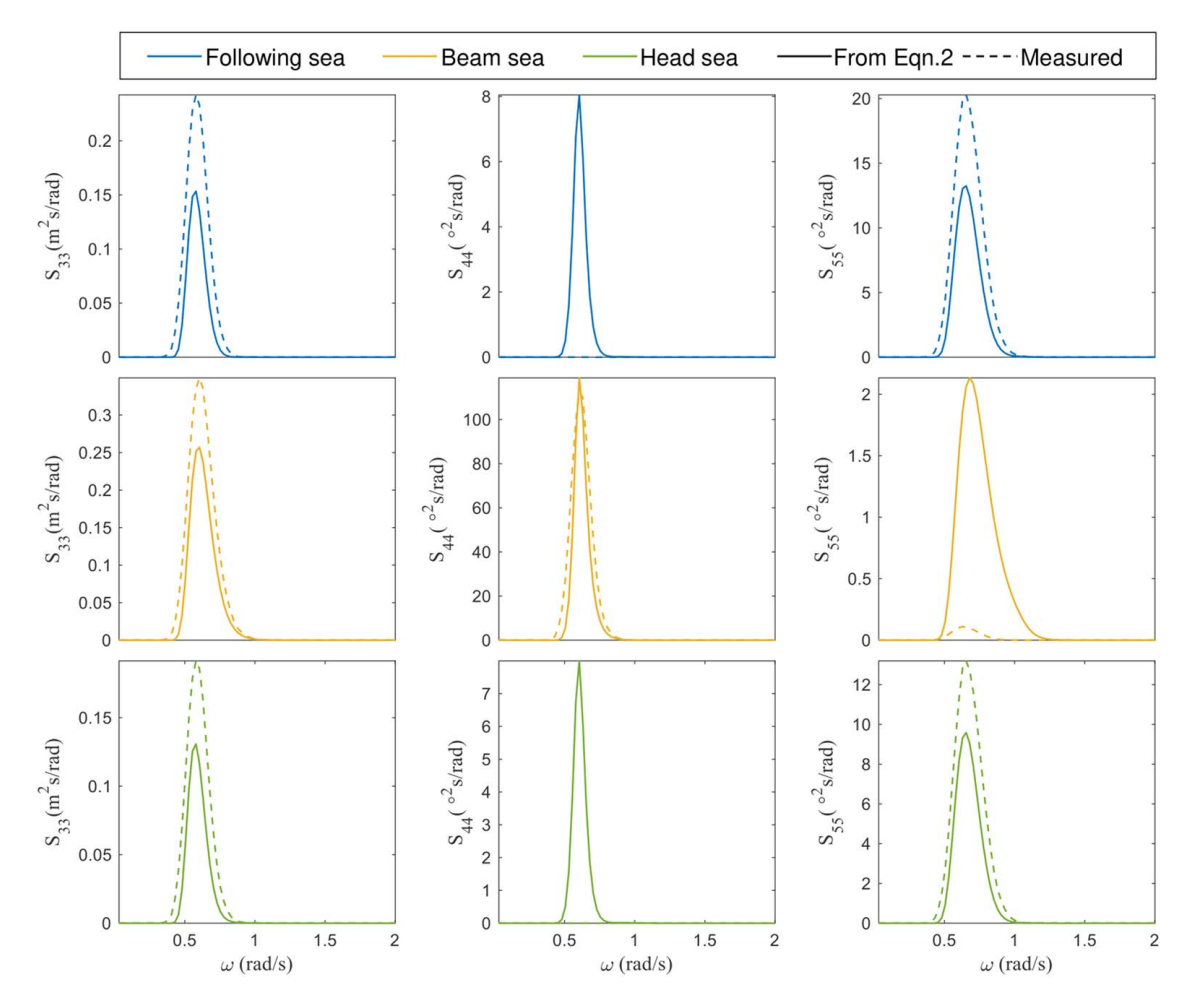


Fig. 3 Ideal response spectra compared with response spectra from measurements

show slightly higher power. A similar phenomenon is observed in head seas (third row), as shown by the green line. In contrast, during beam seas (second row), as indicated by the yellow line, the response power of pitch motion is notably diminished.

**2.4 Performance Deterioration.** In practical applications, the performance of WBA is not consistently reliable due to the uneven energy distribution in the ship's RAOs. For instance, the performance of WBA becomes inferior, since the ship acts as a low-pass filter and filters out high-frequency wave information. The insensitivity to high-frequency waves is inevitable because of the ship's inherent geometry. The performance of WBA also exhibits variations across waves from different directions, e.g., head seas, due to the ship's asymmetric geometry.

In the simulation, a single-peak wave spectrum was used to better demonstrate the proposed performance assessment criterion. The predefined wave spectrum was generated as the product of a JONSWAP spectrum and a spreading function, formulated as follows:

$$E(\omega, \beta) = S(\omega)D(\beta)$$

$$S(\omega) = \frac{H_s^2 \left[ ((4\lambda + 1)/4)\omega_{\mathbf{p}}^4 \right]^{\lambda}}{4\Gamma(\lambda)\omega^{4\lambda+1}} \exp\left[ -\frac{4\lambda + 1}{4} \left( \frac{\omega \mathbf{p}}{\omega} \right)^4 \right]$$

$$D(\beta) = \frac{2^{2s-1}\Gamma^2(s+1)}{\pi\Gamma(2s+1)} \cos^{2s} \left( \frac{\beta - \beta \mathbf{p}}{2} \right)$$
(4)

where  $S(\omega)$  is the long-crest wave spectrum and  $D(\beta)$  is the spreading function.  $H_s$  is the significant wave height,  $\beta_p$  is the mean direction of incoming waves,  $\omega_p$  is the peak wave frequency, and s and  $\lambda$  are

spectrum shape parameters. Ship responses were assumed as the superposition of waves at all considered frequencies and directions, acting on corresponding RAOs, generated from

$$r(t) = \sum_{m=1}^{N_{\omega}} \sum_{n=1}^{N_{\beta}} a_{mn} \cos(\omega_m t + \phi_{mn} + \epsilon_{mn})$$
 (5a)

$$a_{mn} = |\Phi(\omega_m, \beta_n)| \sqrt{2E(\omega_m, \beta_n)\Delta\omega\Delta\beta}$$
 (5b)

$$\phi_{mn} = \arctan\left(\frac{\Im[\Phi(\omega_m, \beta_n)]}{\Re[\Phi(\omega_m, \beta_n)]}\right)$$
(5c)

where  $a_{mn}$  is the motion amplitude of the ship under a specific wave,  $\phi_{mn}$  is the phase of the RAO, and  $\epsilon_{mn}$  is the random phase inherent in waves. The response cross-spectra are obtained using the Welch method, applied over a 900-s period.

As depicted in Fig. 4, the performance of the WBA degrades under the following seas and head seas, where the mean wave heading is oriented at 0 deg and 180 deg. The colorbar below illustrates the distribution of wave energy, with blue (dark) indicating low energy levels and yellow (light) indicating high energy levels. The spectrum shapes of the estimates are dispersed, and the energy is significantly higher than that of the real spectra. Miscalculating sea states can misguide marine operations, resulting in serious consequences. The present study aims to propose an enhanced method to achieve robust sea state estimation.

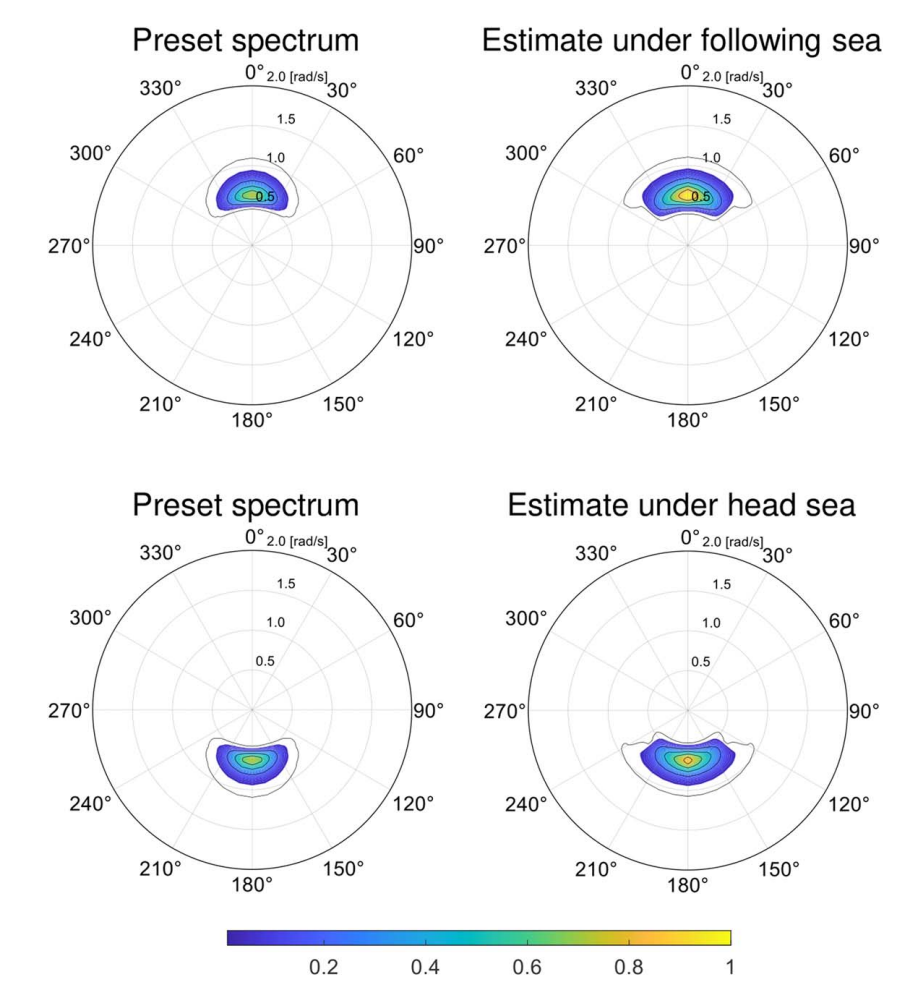


Fig. 4 Performance deterioration of the WBA in special sea states

# 3 Restricted Isometry Property-Based Heading Adjustment

Inaccuracies in WBA estimations can be ascribed to two main sources: power leakage in specific wave headings and performance degradation resulting from unevenly distributed RAOs. In a defined sea state, the DP system can be employed to maintain a vessel's position and heading using its own propellers and thrusters. Therefore, heading adjustment is a viable approach to circumvent inaccuracies in response spectra measurement and achieve an improved estimate. The previous study provides an assessment criterion for evaluating the performance of the wave buoy analogy, using only the ship's RAOs as input. Building on this criterion, the present study introduces a quantitative method for optimal heading adjustment. An illustration of the primary process for incorporating the heading adjustment strategy in sea state estimation is depicted in Fig. 5. The improved estimate is subsequently achieved by adjusting the ship's heading to the orientation that enhances the performance of the WBA.

**3.1 Restricted Isometry Property.** Compressed sensing is a signal processing technique that allows for the recovery of a sparse or compressible signal from a number of measurements smaller than what would traditionally be required. To recover the original sparse signal from measurements, one must solve the illposed problem given by b = Af. Reconstructing the sparse vector f from the measurement matrix A and the measurement vector b is inherently underdetermined. In the WBA, the ill-posed resolution framework and the sparsity of the directional wave spectrum exhibit considerable similarity to the sparse signal recovery process. The accuracy of the reconstruction is contingent upon the RIP of the measurement matrix [24], which can be used to assess the performance of the WBA under specific sea states.

The restricted isometry constant (RIC) serves as a quantitative metric to assess the extent to which a matrix satisfies the RIP condition. Specifically, the kth RIC, denoted by  $\delta_K$ , is defined as the infimum of all possible  $\delta$  for a given matrix  $A \in \mathbb{R}^{m \times n}$ , i.e.,

$$\delta_K := \inf \left\{ \delta : (1 - \delta) \|y\|_2^2 \le \|Ay\|_2^2 \le (1 + \delta) \|y\|_2^2 \quad \forall \, \mathbf{q} \right\}$$
 (6)

The value of RIC is relevant to the eigenvalue of the given matrix A. If a measurement matrix A satisfies the kth RIP with RIC  $\delta_K$ , the following inequality holds:

$$1 - \delta_K \le \lambda_{\min}(A^*A) \le \lambda_{\max}(A^*A) \le 1 + \delta_K \tag{7}$$

where  $\lambda_{\min}(A^*A)$  and  $\lambda_{\max}(A^*A)$  denote the minimal and maximal eigenvalues of  $A^*A$ , respectively. A small value of RIC  $\delta_K$  indicates more accurate signal recovery.

# **3.2 Restricted Isometry Property Apply in Wave Buoy Analogy.** Compressed sensing is a revolutionary technique in data acquisition and signal recovery. It is a mathematical framework that allows for the efficient acquisition and reconstruction of sparse or compressible signals by resolving an inverse problem. The key factors in compressed sensing are the sparse representation of signals and the construction of the measurement matrix. RIP, as defined in (6), is a crucial property for constructing the measurement matrix because it ensures the preservation of the distances between all possible sparse signals [25]. RIC, denoted as $\delta_k$ , is a quantitative measure employed to assess how well a matrix satisfies the RIP condition. A small $\delta_k$ indicates that the measurement process minimally distorts the distances between sparse vectors, which is essential for achieving accurate signal recovery. The RIC is related to the smallest and largest eigenvalues of the measurement matrix.

Estimating the wave spectrum from ship motions exhibits considerable similarity to signal recovery processes. They are both solving an ill-posed inverse problem. The spectral power distribution of waves also shows sparse characteristics because wave energy is concentrated within a narrow range of wave periods and directions.

Hence, the inverse problem of the WBA can be equivalent to signal recovery, and the transfer matrix is equivalent to the measurement matrix in compressed sensing. Instead of a randomly constructed measurement matrix, the transfer matrix in the WBA depends on the RAOs. Unevenly distributed RAOs lead to disparities in the eigenvalues, subsequently affecting the RIC distribution of the transfer matrix. Variations in the RIC distribution explain the discrepancies in computational accuracy across different sea states. Accordingly, the performance deterioration of the WBA can be analyzed from the RIC perspective.

# 3.3 Restricted Isometry Property Evaluation of Transfer Matrix.

#### **Algorithm 1** RIP evaluation

**Input:** Transfer matrix A, sparse order k, number of frequency in selected range  $r_{\omega}$ , sample size  $h_s$ 

**Output:** RIC distribution  $\hat{\delta}$ 

1 Normalize the transfer matrix with a size of  $N_d^2 N_\omega \times N_\beta N_\omega$  into 0-1 interval, denote as A = A/max(abs(A))

```
for n \leftarrow 1 to N_{\beta} do
          for m \leftarrow r_{\omega} + 1 to N_{\omega} - r_{\omega} do
              A_{mn} \leftarrow A[:, nN_{\omega} + m - r_{\omega} : nN_{\omega} + m + r_{\omega}];
5
              n_{col} \leftarrow 2r_{\omega} + 1;
6
               For h \leftarrow 1 to h_s do
                   p \leftarrow \text{RandomPermutation}(n_{col}, k);
8
                   S \leftarrow A_{mn}[:, p];
9
                   \Lambda \leftarrow \text{Eigenvalues}(S^{\top}S);
10
                     if Max(\Lambda) \ge 1 then
                         \delta(h) \leftarrow Max(Max(\Lambda) - 1, 1 - Min(\Lambda)) else
11
12
                             \delta(h) \leftarrow 1 - Min(\Lambda);
13
14
15
                end \hat{\delta}(m,n) \leftarrow \frac{1}{h} \sum_{h=1}^{h_s} \delta(h);
16
17
18 end
```

Rather than utilizing a randomly constructed measurement matrix, the transfer matrix A in the WBA relies on the RAOs. As RAOs are dispersed in an uneven pattern, the eigenvalues are varied, eventually having an effect on the RIC distribution of the transfer matrix. Therefore, examining the WBA's performance degradation from the RIP perspective is thus possible.

To evaluate the accuracy of the WBA estimates, an RIP evaluation algorithm is proposed by calculating the RIC value of the partitioned transfer matrix (as summarized in Algorithm 1). Initially, the transfer matrix formed using RAOs is normalized to an interval of 0 to 1. The sparse order k and frequency range  $r_{\omega}$  are selected in accordance with the power distribution characteristic of the wave spectrum. By traversing various wave directions and frequencies, the block matrix  $A_{mn}$  consists of specific extracted columns from the transfer matrix A.

The RICs of these submatrices are determined using their relationship with the eigenvalues, as formulated in Eq. (7). To ensure the robustness of RIC calculation, number k of the random column sampling method is employed. A measurement matrix with a lower RIC leads to superior signal recovery capacity. Similarly, the RIC of these submatrices signifies how well the transfer matrix satisfies the RIP condition under corresponding sea states. A lower  $\hat{\delta}(m,n)$  denotes better performance under a specific sea state characterized by the peak wave frequency  $\omega_m$  and mean wave direction  $\beta_n$ . Hence, in accordance with the proposed algorithm, the WBA performance can be predicted only based on the RAOs.

An example ship, with geometry parameters detailed in Table 1, was utilized to illustrate the effectiveness of evaluating the WBA

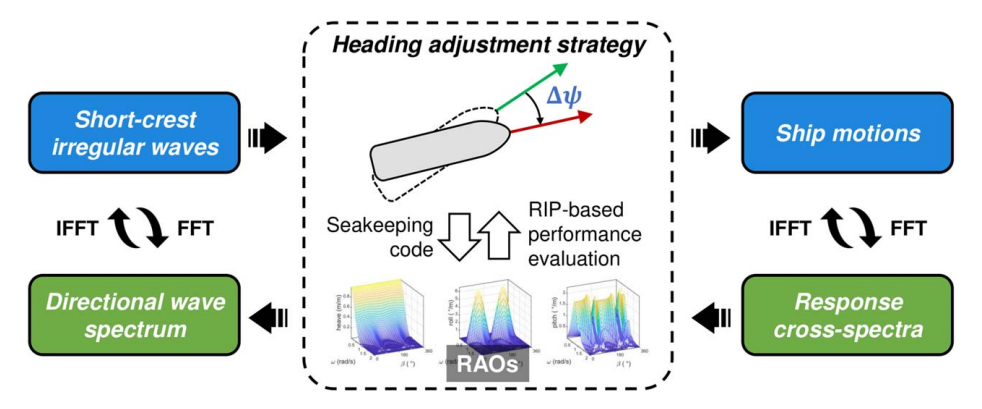


Fig. 5 Overview of the heading adjustment strategy

performance using RIP. The RIC distribution was computed using Algorithm 1, with the sparse order selected as k=10 and a frequency range of  $r_{\omega}=5$ . Subsequently, the RIP distribution corresponding to various sea states is illustrated in Fig. 6(a). A substantial number of simulations were conducted to further validate the consistency in the RIP distribution and WBA performance under various sea states. The analysis takes into consideration the predefined sea state, which includes wave periods ranging from 5 to 15 s and wave directions ranging from 0 deg to 360 deg. To eliminate errors from inaccurate response cross-spectra, the ideal response spectra were employed in the case study. Mean square error (MSE) was employed to measure the estimation error of the WBA with ideal responses, compared with the actual predefined sea states, given by

$$MSE = \frac{1}{N_{\omega}N_{\beta}}|f - \hat{f}|^2$$
 (8)

where f and  $\hat{f}$  represent the WBA estimate and real wave spectrum in vector form, respectively. The WBA error distribution is depicted in Fig. 6(b).

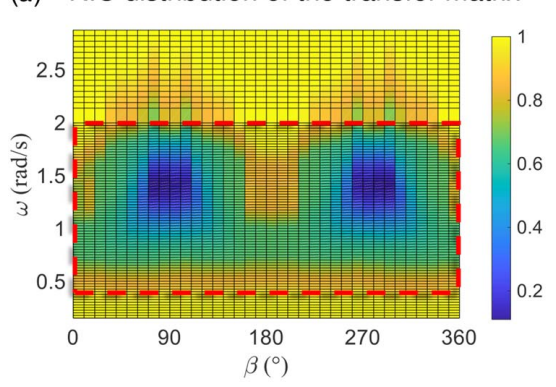
It is noteworthy to observe that RIC values increased and approached a value of 1 when encountering waves of both high and low frequencies, indicating suboptimal WBA performance in the corresponding sea states (see Fig. 6(a)). Furthermore, the RIC exhibits relatively high values in head seas and following seas, i.e.,  $\beta$  approaches 180 deg and 0 deg/360 deg, aligning with the previously mentioned performance deterioration. Comparing Fig. 6(a) and Fig. 6(b), the patterns observed in the distributions of estimation errors are consistent with the distribution of RIC values (corresponding wave parameters were framed in red). The performance is inferior under extremely high-frequency and low-frequency waves, and there are increasing errors in the head and following

**3.4 Heading Adjustment Strategy.** The WBA has demonstrated its capability to identify the primary characteristics of wave energy in a substantial number of simulations. This implies that the peak wave frequency  $\omega_m$  and mean wave direction  $\beta_n$  can be accurately determined. In specific sea states (such as head seas, beam seas, and following seas), power leakage may occur,

Table 1 Geometry and hydrostatic parameters of the example cargo ship

(m)	55, 12, 4
$(m^3)$	995
(m)	6.5
$(m^2)$	568
$(kg m^2)$	15,979,178
$(kg m^2)$	123,296,000
$(kg m^2)$	123,296,000
	(m <sup>3</sup> ) (m) (m <sup>2</sup> ) (kg m <sup>2</sup> ) (kg m <sup>2</sup> )

## (a) RIC distribution of the transfer matrix



## (b) MSE distribution of the WBA estimates

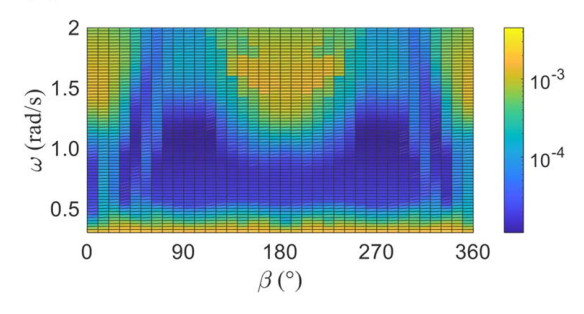


Fig. 6 RIC distribution of the transfer matrix and MSE distribution of the WBA under various sea states

as mentioned earlier. The reliability of the current estimate can be characterized using the RIC distribution derived from Algorithm 1. DP ships are commonly used in marine operations, with heading adjustment being a feasible application within the DP system. The appropriate heading adjustment angle can be determined by avoiding specific wave headings, allowing the ship to achieve better performance estimation by relying on the RIC distribution.

The two-step strategy is summarized in Fig. 7. The inputs are special wave headings collected in a set  $\{\beta_s\}$ , threshold  $\bar{\delta}$  of RIC, and adjustment range r based on the DP system and operational considerations. The special wave heading is defined as  $\beta_s = \{\beta \in [\beta_o - \Delta\beta, \ldots, \beta_o + \Delta\beta] | \beta_o = 0, 90, 180, 270\}$  and  $\Delta\beta = 10 \deg$ . The initial step involves identifying the peak wave frequency  $\omega_{peak}$  and mean wave direction  $\beta_{peak}$  of the current sea state, indexed by  $m_p$  and  $m_p$ , respectively. If the ship is found within the specific inferior sea state, preset as an input to the algorithm and potentially result in inaccurate response spectra, heading adjustment becomes imperative. In cases where the ship is not

within such range, the RIC value is employed to assess the reliability of the current estimate. If the corresponding RIC  $\delta(m_p,n_p)$  surpasses the predefined threshold  $\bar{\delta}$ , heading adjustment is deemed necessary. Conversely, if the RIC value remains below the threshold, the algorithm considers the current estimate as reliable. In instances where heading adjustment is required, the rotation angle  $\Delta \psi$  is determined by searching for the lowest RIC value within the preset adjustment range. If  $\Delta \psi = 0$ , the current heading direction provides the optimal estimate within the limitations of frequency capture capacity and heading adjustment range. Otherwise, the estimate  $\hat{E}$  is ultimately obtained after the heading rotation.

#### 4 Simulation and Result

To demonstrate the efficacy of the proposed heading adjustment strategy, a series of simulations were implemented, utilizing a cargo ship with the geometry and main hydrostatic parameters detailed in Table 1. The sea state definition and ship's responses were the same as the process detailed in Sec. 2.4. The RAOs of the ship were assumed to be perfectly known, derived from potential flow theory. To initialize the heading adjustment strategy, the threshold  $\bar{\delta}$  was established at 0.75 and the heading adjustment range was chosen as 40 deg, i.e., r=4. Predefined sea states were generated through Eq. (4) by randomly selecting wave parameters. The directional wave spectra were discretized into  $36 \times 100$  grids, encompassing  $N_{\beta}=36$  directions and  $N_{\omega}=100$  frequencies. A stationary sea state was assumed throughout the 900-s simulation period. The generated time series and the calculated cross-response spectra are shown in Fig. 8, with the simulation requiring only 3 s to execute on an Intel Core i7-12700 computer.

Several simulations were illustrated to showcase the effectiveness of the heading adjustment strategy. In Fig. 9, the vessel encountered the following seas, and the original estimate displays

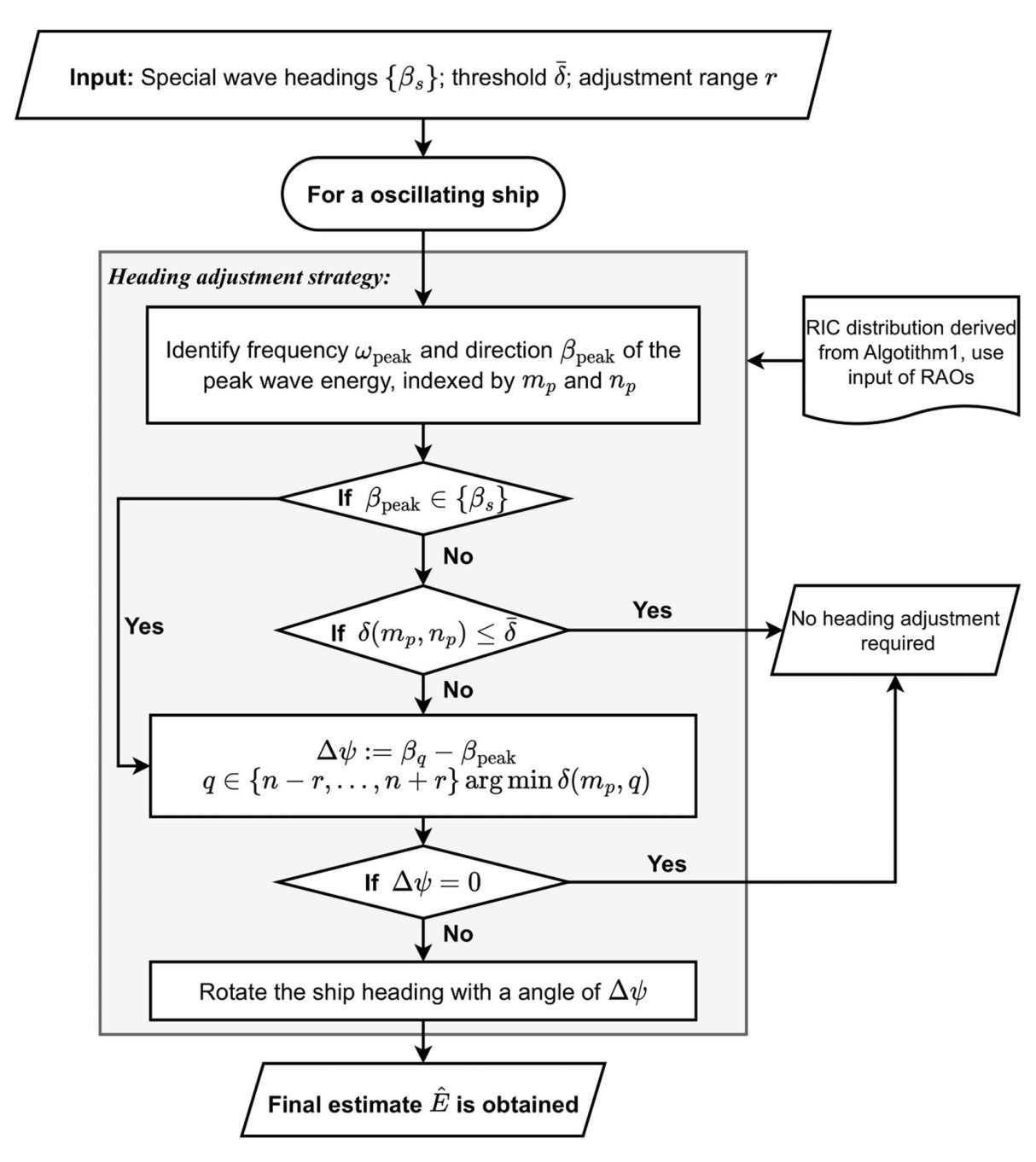


Fig. 7 Flowchart of the heading adjustment strategy

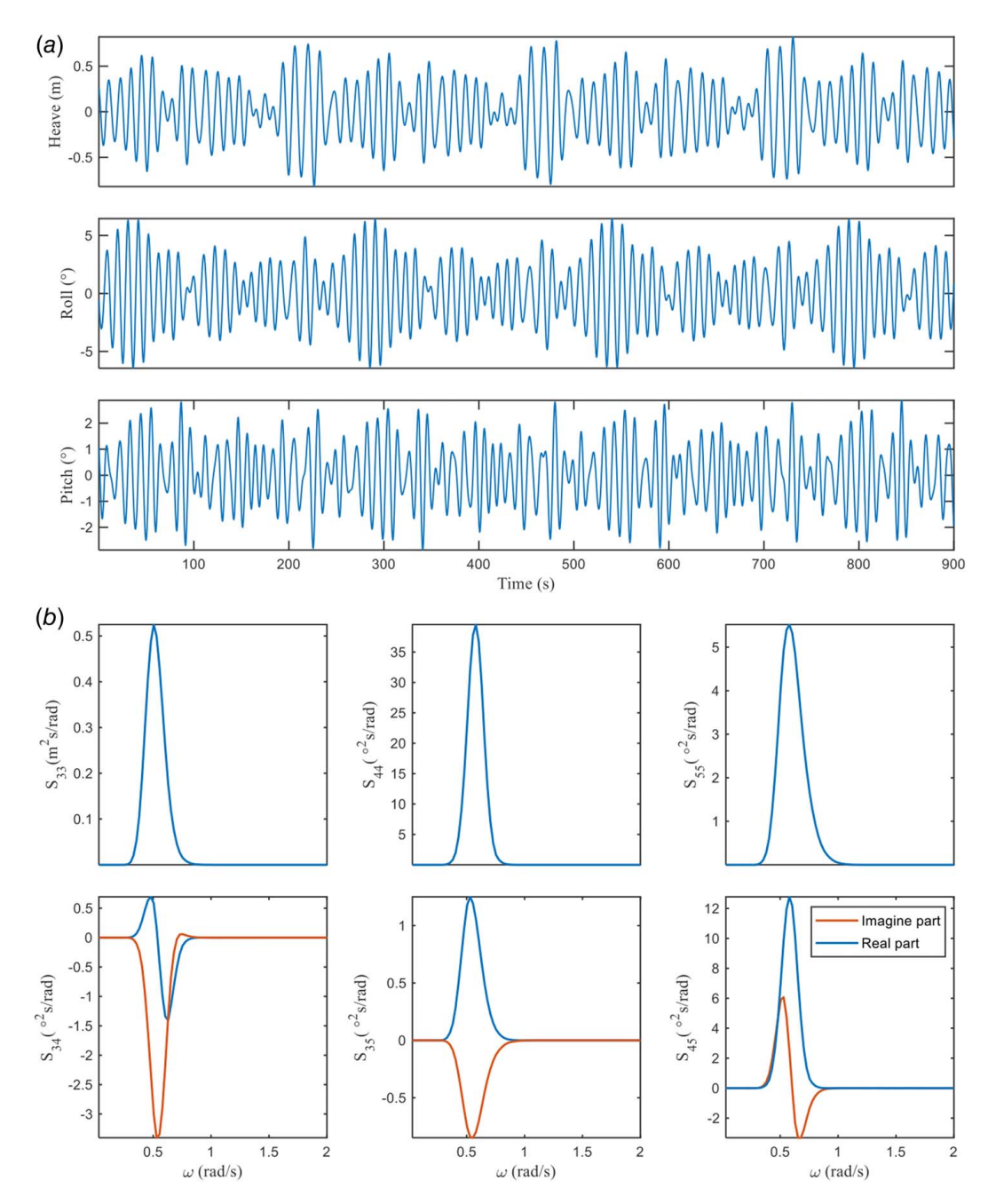


Fig. 8 Generated time series and the cross-response spectra

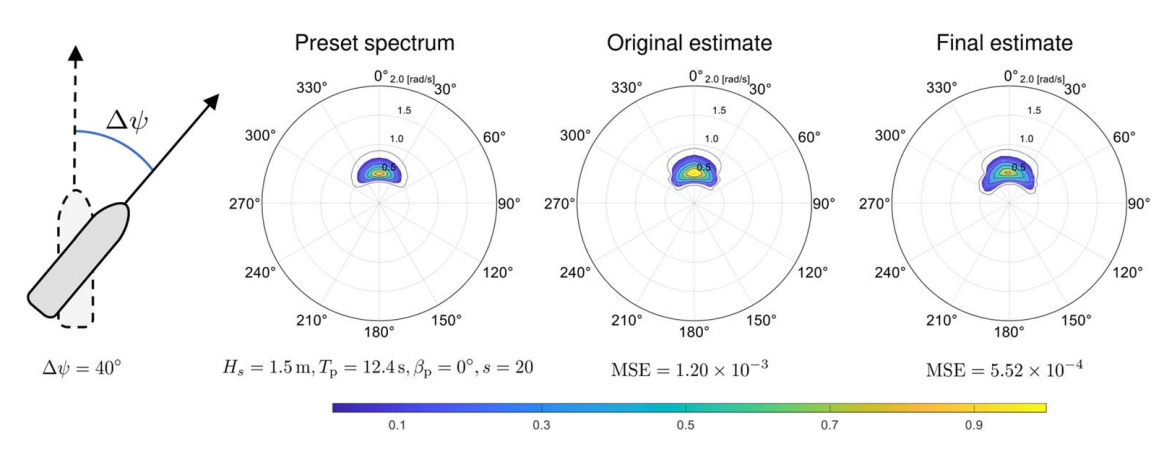


Fig. 9 Simulation result under sea state 1

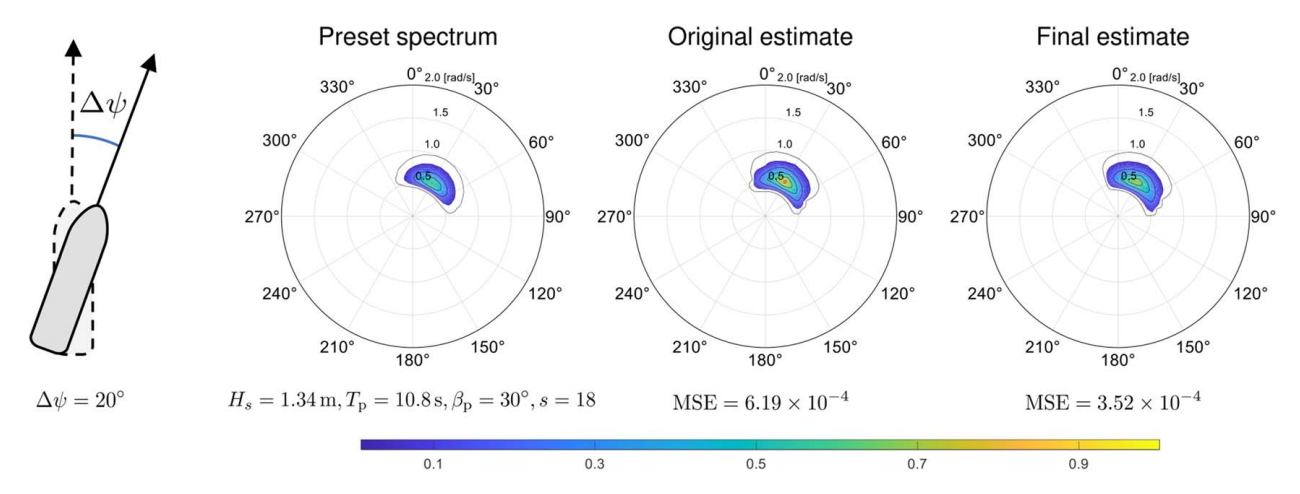


Fig. 10 Simulation result under sea state 2

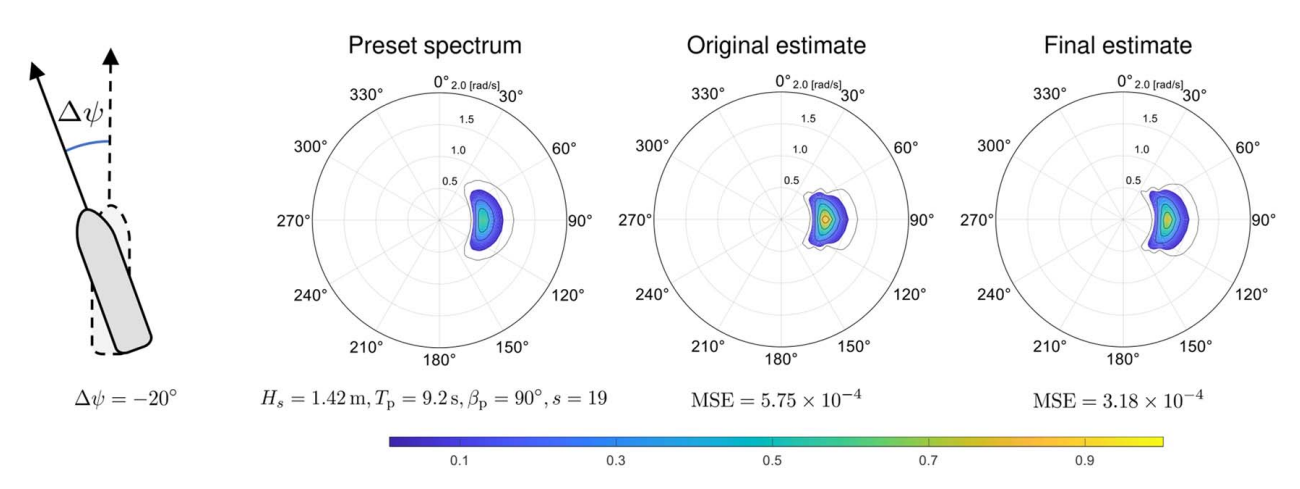


Fig. 11 Simulation result under sea state 3

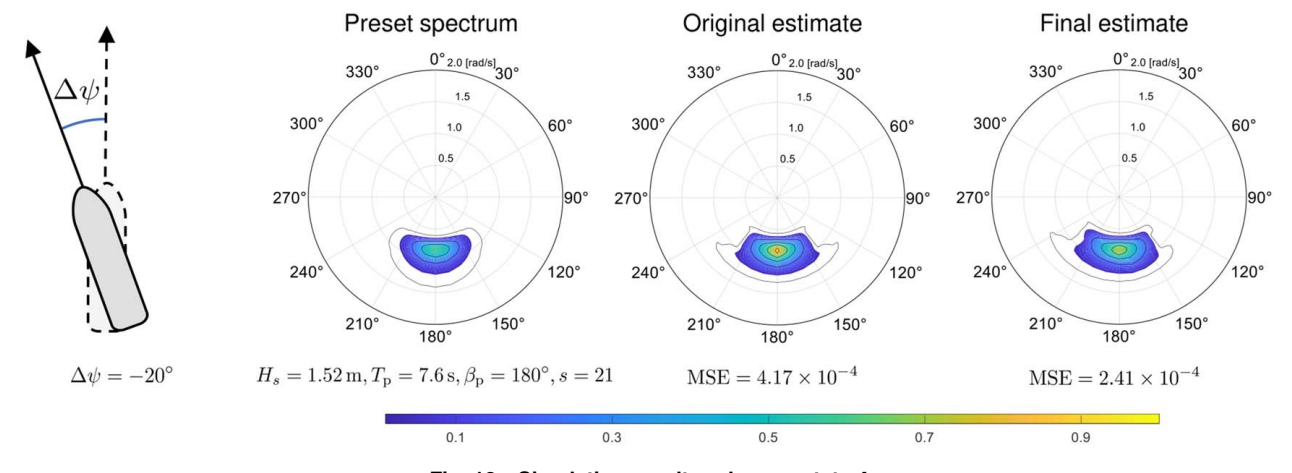


Fig. 12 Simulation result under sea state 4

a notably higher energy distribution along with a substantial MSE. Following the strategy, a heading adjustment of  $\Delta \psi = 40\,\mathrm{deg}$  is deemed necessary. Subsequent to the adjustment of the ship's heading, the estimate is refined, resulting in a noteworthy decrease in MSE. As depicted in Fig. 10, the adjustment is also required, ultimately leading to an improved estimate for the ship. In Fig. 11, when the ship originally encounters beam seas, the heading adjustment strategy intervenes, resulting in a change in the ship's heading. The initially higher and concentrated wave spectrum estimation is also significantly ameliorated. In head seas, as illustrated in

Fig. 12, the effectiveness of the heading adjustment strategy becomes evident, accompanied by a reduction in MSE.

Through simulations conducted under diverse sea conditions, it became feasible to visually observe performance improvements where the heading adjustment strategy intervened. Due to the vessel's symmetry geometry, the simulation was conducted only for cases within 0–180 deg. The results of parameter sweeping are presented in Fig. 13, wherein the yellow (lighter) blocks indicate the need for heading adjustment, while the gray (darker) blocks show that no adjustment is required. Under specific incoming

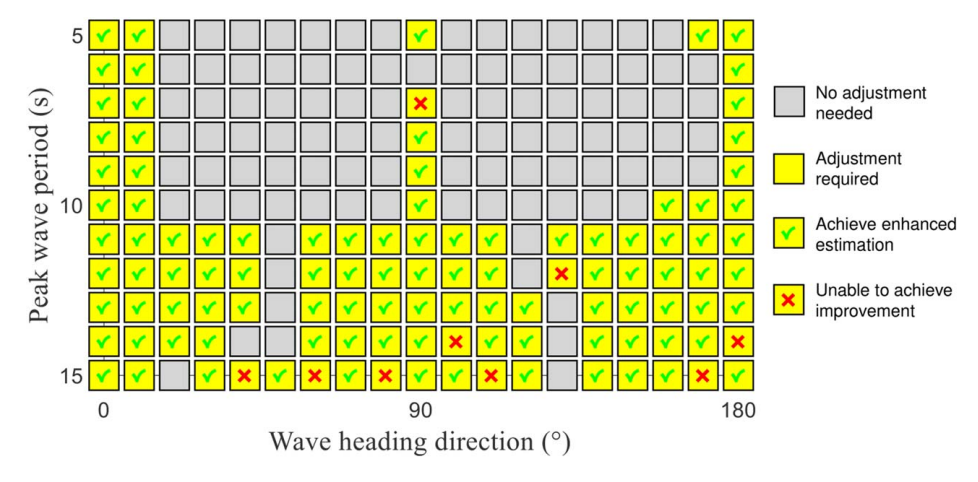


Fig. 13 Effectiveness of the adjustment strategy under a parameter sweeping

wave angles and low-frequency sea states (with peak wave periods longer than 10 s), the proposed method increasingly contributes to sea state estimation. In the majority of cases, the inclusion of a heading adjustment strategy can improve estimates. However, there are exceptions, particularly in extreme low-frequency waves. This occurs because ships act as low-pass filters in ocean waves, exhibiting little to no response to waves that exceed their response threshold. Therefore, in waves with a period of 15 s, heading adjustments cannot enhance performance due to the ship's inherent properties. In some cases, where improvements are not achievable, the results may be comparable to the original estimates without deterioration.

#### 5 Conclusion

This study addresses two key contributors to inaccurate sea state estimation: power leakage in specific wave headings and performance degradation in specific sea states due to the ship's uneven hydrodynamics. To mitigate these issues, a quantitative heading adjustment strategy is proposed, aiming to avoid inaccuracies in cross-spectra and determine the optimal adjustment angle. The RAO-driven strategy is grounded in the RIP-based WBA performance assessment. A substantial number of simulations were conducted to validate the consistency between the RIC distribution and estimation errors. Additionally, several cases were presented to illustrate the effectiveness of the proposed heading adjustment strategy. Parameter sweeping further confirmed the improvements resulting from the heading adjustment.

Several limitations exist in the presented method. Due to the inherent low-pass characteristics of ships, adjustments in heading may not enhance measurements when encountering low-frequency waves. The model-based WBA and the proposed assessment criterion are predicated on the assumption that the RAOs can accurately represent the wave–ship interaction pattern. Consequently, the robustness of the method must be improved to decrease reliance on an ideal RAO. The scope of the heading adjustment method is constrained by the seakeeping assumption. The ship's heading during navigation cannot be arbitrarily adjusted, and the occurrence of Doppler shift is another consideration. Furthermore, sea trial data are necessary to further demonstrate the effectiveness of the approach.

## Acknowledgment

This work was supported by Natural Science Foundation of Guangdong Province, China (Grant No. 2024A1515011731) and Shenzhen Science and Technology Program, China (Grant No. KJZD20231023100459001).

#### Conflict of Interest

There are no conflicts of interest.

### **Data Availability Statement**

The datasets generated and supporting the findings of this article are obtainable from the corresponding author upon reasonable request.

#### Nomenclature

b = response spectra in vector form

f =directional wave spectrum in vector form

r = adjustment range

A = transfer matrix in WBA

E = directional wave spectrum

S = response cross-spectra

 $x^*$  = Hermite transpose of x

i, j = index of DOFs

 $_m$  = index of wave frequencies

n =index of wave directions

||x|| = norm of x

 $\overline{x} = \text{complex conjugate of } x$ 

 $\beta$  = wave heading angle (deg)

 $\delta$  = value of RIC

 $\Phi$  = transfer function

 $\psi$  = ship heading angle (deg)

 $\omega$  = angular wave frequency (rad/s)

#### References

- Wang, S., Moan, T., and Gao, Z., 2025, "Time-Domain Fatigue Analysis Methodology for Semi-submersible Hulls of Floating Wind Turbines." Available at SSRN 5080108.
- [2] Fu, J., Shi, W., Han, X., Karimirad, M., Wang, T., and Li, X., 2025, "Development and Performance Study of a Multi-degree-of-freedom Loading Device for Real-Time Hybrid Model Testing of Floating Offshore Wind Turbines," Marine Struct., 99, p. 103717.
- [3] Ma, C., Zhang, T., Jiang, Z., and Ren, Z., 2025, "Dynamic Analysis of Lowering Operations During Floating Offshore Wind Turbine Assembly Mating," Renew. Energy, 243, p. 122528.
- [4] Chen, M., Huang, W., Liu, H., Hallak, T. S., Liu, S., Yang, Y., Tao, T., and Jiang, Y., 2025, "A Novel SPM Wind-Wave-Aquaculture System: Concept Design and Fully Coupled Dynamic Analysis," Ocean Eng., 315, p. 119798.
- [5] Guo, Y., and Alam, M., 2025, "Nonlinear Bending and Thermal Postbuckling of Magneto-electro-elastic Nonlocal Strain-Gradient Beam Including Surface Effects," Appl. Math. Model., 142, p. 115955.
- [6] Dam Nielsen, U., 2006, "Estimations of On-Site Directional Wave Spectra From Measured Ship Responses," Mar. Struct., 19(1), pp. 33–69.
- [7] Newman, J. N., 2018, Marine Hydrodynamics, The MIT Press.
- [8] Iseki, T., and Ohtsu, K., 2000, "Bayesian Estimation of Directional Wave Spectra Based on Ship Motions," Control Eng. Pract., 8(2), pp. 215–219.

- [9] Nielsen, U. D., and Dietz, J., 2020, "Ocean Wave Spectrum Estimation Using Measured Vessel Motions From an In-service Container Ship," Marine Struct., 69, p. 102682.
- [10] Mas-Soler, J., and Simos, A. N., 2020, "A Bayesian Wave Inference Method Accounting for Nonlinearity Related Inaccuracies in Motion RAOs," Appl. Ocean Res., 99, p. 102125.
- [11] Pascoal, R., Perera, L. P., and Guedes Soares, C., 2017, "Estimation of Directional Sea Spectra From Ship Motions in Sea Trials," Ocean Eng., 132, pp. 126–137.
- [12] Kim, H., Kang, H., and Kim, M.-H., 2019, "Real-Time Inverse Estimation of Ocean Wave Spectra From Vessel-Motion Sensors Using Adaptive Kalman Filter," Appl. Sci., 9(14), p. 2797.
- [13] Peng, X., Zhang, B., and Rong, L., 2019, "A Robust Unscented Kalman Filter and Its Application in Estimating Dynamic Positioning Ship Motion States," J. Marine Sci. Technol., 24(4), pp. 1265–1279.
- [14] Ren, Z., Han, X., Verma, A. S., Dirdal, J. A., and Skjetne, R., 2021, "Sea State Estimation Based on Vessel Motion Responses: Improved Smoothness and Robustness Using Bézier Surface and L1 Optimization," Marine Struct., 76, p. 102904.
- [15] Chen, Y., Ding, Y., Hu, Z.-Z., and Ren, Z., 2025, "Geometrized Task Scheduling and Adaptive Resource Allocation for Large-Scale Edge Computing in Smart Cities," IEEE Int. Things J., pp. 1–1.
- [16] Nelli, F., Derkani, M. H., Alberello, A., and Toffoli, A., 2023, "A Satellite Altimetry Data Assimilation Approach to Optimise Sea State Estimates From Vessel Motion," Appl. Ocean Res., 132, p. 103479.
- [17] Toffoli, A., Alberello, A., Clarke, H., Nelli, F., Benetazzo, A., Bergamasco, F., Ntamba, B. N., Vichi, M., and Onorato, M., 2024, "Observations of Rogue Seas in the Southern Ocean," Phys. Rev. Lett., 132(15), p. 154101.

- [18] Tu, F., Ge, S. S., Choo, Y. S., and Hang, C. C., 2018, "Sea State Identification Based on Vessel Motion Response Learning Via Multi-layer Classifiers," Ocean Eng., 147, pp. 318–332.
- [19] Kawai, T., Kawamura, Y., Okada, T., Mitsuyuki, T., and Chen, X., 2021, "Sea State Estimation Using Monitoring Data by Convolutional Neural Network (CNN)," J. Marine Sci. Technol., 26(3), pp. 947–962.
- [20] Han, P., Li, G., Skjong, S., Wu, B., and Zhang, H., 2021, "Data-Driven Sea State Estimation for Vessels Using Multi-domain Features From Motion Responses," 2021 IEEE International Conference on Robotics and Automation (ICRA), Xi'an, China, pp. 2120–2126.
  [21] Li, S., Cheng, X., Shi, F., Zhang, H., Dai, H., Zhang, H., and Chen, S., 2024, "A
- [21] Li, S., Cheng, X., Shi, F., Zhang, H., Dai, H., Zhang, H., and Chen, S., 2024, "A Novel Robustness-Enhancing Adversarial Defense Approach to AI-Powered Sea State Estimation for Autonomous Marine Vessels," IEEE Trans. Syst. Man Cybernet: Syst., 55(1), pp. 28–42.
- Cybernet: Syst., **55**(1), pp. 28–42.
  [22] Han, P., Li, G., Skjong, S., and Zhang, H., 2022, "Directional Wave Spectrum Estimation With Ship Motion Responses Using Adversarial Networks," Marine Struct., **83**, p. 103159.
- [23] Zhang, T., and Ren, Z., 2025, "Restricted Isometry Property in Wave Buoy Analogy and Application to Multispectral Fusion," IEEE Trans. Intell. Transp. Syst., 26(2), pp. 1999–2010.
- [24] Davenport, M. A., Duarte, M. F., Eldar, Y. C., and Kutyniok, G., 2012, "Introduction to Compressed Sensing," *Compressed Sensing: Theory and Applications*, G. Kutyniok, and Y. C. Eldar, eds, Cambridge University Press, Cambridge, pp. 1–64.
- [25] Candès, E. J., Romberg, J. K., and Tao, T., 2006, "Stable Signal Recovery From Incomplete and Inaccurate Measurements," Commun. Pure Appl. Math., 59(8), pp. 1207–1223.